



Published in final edited form as:

ACS Med Chem Lett. 2013 August 8; 4(8): 762–767. doi:10.1021/ml400166b.

Synthesis and Metabolic Studies of Host Directed Inhibitors for Anti Viral Therapy

Terry W. Moore[†], Kasinath Sana[†], Dan Yan[§], Stefanie A. Krumm[§], Pakh Thepchatri[†], James P. Snyder^{†,μ}, José Marengo[†], Richard F. Arrendale[†], Andrew J. Prussia[†], Michael G. Natchus[†], Dennis C. Liotta^{†,μ}, Richard K. Plempner^{§,ν}, and Aiming Sun^{*,†}

[†]Emory Institute for Drug Development, Yerkes National Primate Research Center, Emory University, 954 Gatewood Rd., NE Atlanta, GA 30329, USA

[§]University Center for Inflammation, Immunity & Infection, Georgia State University, Atlanta, GA 30303, USA

^μDepartment of Chemistry, Emory University, 1515 Dickey Drive, Atlanta, GA 30322, USA

^νDepartment of Pediatrics, Emory University School of Medicine, 2015 Uppergate Drive, Atlanta, GA 30322, USA

Abstract

Targeting host cell factors required for virus replication provides an alternative to targeting pathogen components and represents a promising approach to develop broad-spectrum antiviral therapeutics. High-throughput screening (HTS) identified two classes of inhibitors (**2** and **3**) with broad-spectrum antiviral activity against ortho- and paramyxoviruses including influenza A virus (IAV), measles virus (MeV), respiratory syncytial virus (RSV), and human parainfluenza virus type 3 (HPIV3). Hit-to-lead optimization delivered inhibitor, **28a**, with EC₅₀ values of 0.88 and 0.81 μM against IAV strain WSN and MeV strain Edmonston, respectively. It was also found that compound **28a** delivers good stability in human liver S9 fractions with a half-life of 165 minutes. These data establish **28a** as a promising lead for antiviral therapy through a host-directed mechanism.

Keywords

Myxovirus inhibitor; host-directed; influenza A; respiratory syncytial virus; benzimidazole; metabolic stability

The orthomyxovirus and paramyxovirus families comprise many pathogens that cause common respiratory illnesses; among them are measles virus, mumps virus, respiratory syncytial virus, human parainfluenza virus (paramyxoviruses) and influenza viruses A and B (orthomyxoviruses). Together, the acute respiratory illnesses caused by these viruses represent a major medical need.¹ In particular, the likelihood of pandemic from influenza A makes developing new and broadly active therapies a pressing global need.² Our research group has undertaken a program of discovering and developing antivirals that target host factors implicated in virus reproduction. Although this runs counter to the prevailing virus-targeted mechanistic approach to discovering antivirals, the potential benefits of such a

*To whom correspondence should be addressed: Phone: 404-727-4860; asun2@emory.edu.

Supporting Information. Experimental details for the synthesis and characterization of **2**, **2a-h**, and **3-32**. Experimental details for biology assays. This material is available free of charge via the Internet at <http://pubs.acs.org>.

strategy include decreased incidence of resistance, because host factors mutate less readily than viral factors, and a broadened spectrum of antiviral activity, because many of the same host factors are co-opted by different viruses.^{3, 4} A potential drawback to this approach is the nontrivial efforts required to define mechanism of action, since we use a whole-cell phenotypic screen to identify these antivirals.⁵ To date, our most successful compound series has been exemplified by the broadly active benzimidazole **1** (JMN3-003), which has low nanomolar activity against a number of different viruses in cell culture.^{6, 7} In our efforts to develop a backup to **1**, we have re-examined two different hits (scaffolds **2** and **3**, Figure 1) that were described in the same high-throughput screening paper in which we first disclosed benzimidazole **1**.⁵ This report details our attempts to simultaneously improve potency against both an orthomyxovirus (influenza A) and paramyxovirus (measles) representative and to understand the metabolic profile in liver S9 fractions for **2** and **3**.

To confirm the biological activity of series **2** and **3**, these two hits along with a small set of analogs were synthesized, and tested in reporter gene assays. In the case of IAV assays, a firefly luciferase minireplicon reporter was driven by superinfection of cells with influenza A/sw/Texas/2009 or influenza A/Aichi/1968. 50% -inhibitory concentrations were calculated by means of four-parameter non-linear regression-fitting; values in parentheses represent 95% confidence intervals. Syntheses of **2** and closely related analogs were initiated by treatment of commercially available benzimidazolylacetonitrile (**4**) with sodium nitrite in acetic acid. The resulting cyano oxime **5** was combined with hydroxylamine and cyclized to afford furazan **6**. The latter was further coupled with acyl chlorides **7** to deliver **8**, followed by alkylation to give compound **2** and its analogs (Scheme 1). Analogues with a thiazole, pyrazole, or pyrazine instead of the furazan moiety, were also synthesized (Scheme 2 - 5, SI).

Compound **2** and analogs were re-tested against both IAV and MeV. Replacement of the ethyl ester with a 4-aminophenyl moiety (**2b**) led to a slight loss of activity, while replacement with hydrogen caused a complete loss of potency against both viruses (**2a**). All series **2** analogs featuring an altered central ring system lost bioactivity (**2c-g**, Table 1). Active compounds **2** and **2b** were subjected to further chemical and metabolic stability testing against human and hamster liver S9 fractions ($T_{1/2} < 5$ min in presence or absence of cofactors). Although the potency of compound **2** is good, we speculate that the biological activity of this compound might arise from its metabolic or chemical instability, which ultimately led us to drop pursuit of this series in favor of alternative scaffold **3**.

The syntheses of analogs of **3** were modified based on the procedures of Laufer *et al.*⁸ Briefly, 4,5-diphenyl-2-thioimidazole was treated with alkyl bromides to give thioethers **10**. The thioether was either oxidized to the sulfone **11** first and alkylated⁹ or, alternatively, alkylated and then oxidized to yield **13**.¹⁰ Deprotonating the benzylic α -carbon and fluorinating once or twice gave analogs **14a** and **14b**. (Scheme 2)

To obtain differentially substituted analogs, the acetophenones **15** were brominated (**16**), coupled with methylamine, and acidified to give α -ammonium ketones **17**.⁸ These analogs were cyclized using sodium thiocyanate to give the thioimidazoles **18**.^{8, 11} Alkylation delivered the thioethers **19**, and bromination gave the 5-bromoimidazoles **20**.^{8, 12} *m*CPBA oxidation provided the sulfone **21**, and Suzuki coupling yielded the tetra-substituted imidazoles **22** (Scheme 3). The synthesis of **28a** and analogs is shown in Scheme 4 starting with treatment of 1-methyl-4,5-diphenylimidazole **29** with *n*-butyllithium and DMF to afford 2-formyl imidazole **30**.¹³ Reductive amination of **30** with different aromatic amines delivered amines **31**, which underwent either a second reductive amination with formaldehyde or benzaldehyde or LiHMDS-mediated alkylation to furnish **28a-d**, respectively.

In exploring the SAR around **3**, we found that replacing the propargyl group with a hydrogen atom (**13a**) or a benzyl group (**13e**) led to a complete loss of potency against both IAV and MeV (**13a**), replacement with an ethyl (**13d**) or allyl group (**13f**) led to reduced potency, and replacement with a methyl group (**13b**) yielded analogs with comparable potency to unmodified **3** against influenza, particularly, indicating a preference for small alkyl substituents at the 1-position. Trifluoro analog **13c** was synthesized and found to have reduced potency against IAV and MeV as compared to **3**. In an attempt to increase potency, solubility, and metabolic stability, two of the three phenyl rings were independently replaced with pyridine (**13g**, **13h**), and both compounds completely lost activity.

Having demonstrated promising activity within this series, we turned our attention to the metabolic stability of the compounds. We assayed a subset of the compounds for metabolic stability in human and hamster liver S9 fractions, the latter species chosen for its likely use in a potential efficacy study. We selected a panel of compounds for this study to probe likely metabolic transformations: nucleophilic addition into the heterocyclic sulfone and subsequent elimination of the sulfinate, oxidation of the aromatic rings, oxidation of the *N*-alkyl group, or oxidation of the methylene group α to the sulfonyl. While rapidly metabolized in pooled hamster liver S9 fractions ($T_{1/2} < 2.5$ min), compounds **3**, **13a**, and **13b** showed a slightly prolonged half-life in the pooled human liver S9 fractions with half-lives of 19, 14, and 2-12 min, respectively (Table 2). Surprisingly, the tris-fluorophenyl analog **13c** showed rapid breakdown in human and hamster liver S9 fractions with both half-lives less than 2.5 min (Table 2). Common to these four analogs is a sulfonylmethylene moiety, which links the left-most imidazole and right-most aryl rings of the molecule, presenting a potential metabolic instability. We observed no metabolism in the absence of cofactors, implying that the compounds were chemically stable and that elimination of the sulfone as a sulfinate, were it to occur, must be cofactor-mediated. Towards understanding the role of the methylene carbon in the metabolism, we introduced one or two fluorines into the molecule at the methylene carbon. Although incorporation of one fluorine at that position (**14a**) conferred no additional S9 stability, introduction of a second fluorine (**15**) resulted in good stability in pooled hamster S9 fractions ($T_{1/2} = 54$ min) and excellent stability in the human system ($T_{1/2} > 90$ min). These results suggest that the sulfonylmethylene represents a substantial metabolic liability for this compound class (Table 2).

We attempted to determine the identity of the metabolite(s) using LC-MS/MS. After incubating **13b** (100 μ M) with pooled human liver S9 fractions for 20 minutes, we observed a peak (91% of total area) in the LC-MS that corresponded to a mass with m/z of 576 (+187 Da) and 531 (+142 Da; data not shown). Enhanced Product Ion (EPI) of the metabolite with m/z 576 produced a fragment with m/z 298 which is consistent with the mass of the 4,5-diphenylimidazole sulfone structure. Taken together, these data are consistent with our hypothesis of an unstable species, perhaps a reactive metabolite that arises from hydrolysis of an α -hydroxysulfone intermediate or a product of secondary metabolism.

Unfortunately, having repaired the metabolic liability in **13b**, we found that fluorinating the metabolically labile methylene resulted in complete loss of antiviral activity (**14b** and **15**, Table 3). Understanding this key weakness within the molecule, we replaced the sulfonylmethylene moiety altogether with a variety of two-atom linkers. Replacing the sulfone with a thioether moiety led to analog **12**, which exhibited not only reduced anti-viral activity against IAV, but also shortened compound half-life in both hamster and human liver S9 fractions (**12**, Table 3), a curious finding when one considers the difference in electron density at the α -carbons of **13a** and **12**. Further modification by replacing the sulfone with a carbonyl group led to analog **25**, which showed much improved stability in human liver S9 fractions (human S9 $T_{1/2} > 90$ min) but diminished potency (Table 3). Replacing the

sulfonylmethylene with a sulfonamide (**23**) or a 1,2-disubstituted ethanol (**26**) caused not only complete loss of activity but also failed to confer metabolic stability. Compounds **24a** and **24b**, in which an amide linker replaces the sulfonylmethylene, were about 100 fold less potent than compound **3**. A similar result was found with replacement by an ethane linker (**27**, Table 3). Strikingly, we found analog **28a**, with an aminomethyl linker, to return good potency with EC₅₀ values of 0.88 μM against IAV-WSN and 0.81 μM against MeV-Edm. Compound **28a** was also found to be metabolically stable in pooled human liver S9 fractions with a half-life of 165 min. While the potency and metabolic stability of **28a** are very promising, the solubility of **28a** is quite poor (<15 μg/mL at pH=7.4). We attempted to address this issue by either generating salts of **22** or incorporating hydrophilic groups in the right-hand portion of the molecule. Compound **28b** with a hydroxyl group, **28c** with a carboxyl group, and **28d** with pyridine instead of a phenyl ring, were synthesized and subjected to solubility testing based on nephelometry. Analog **28c** showed superb solubility of greater than 300 μg/mL at pH=7.4 (Table 3).

In conclusion, we have described two new series of analogs that may have broad-spectrum anti-myxovirus activity, albeit with higher EC₅₀ values than with our previously reported scaffold **1**.^{6, 7, 14} While the first of these series, based on furazan **2**, delivered potent compounds, this series was chemically and metabolically unstable. The second series, based on imidazole **3**, yielded bioactive compounds that were compromised, however, by metabolic liabilities likely arising from the benzylic methylene group α to the sulfone. Replacing the sulfonylmethylene with a methyleneamine moiety leads to a bioactive (EC₅₀ value for **28a** approximately 0.8-0.9 μM against different myxovirus family members) and metabolically stable analog (human S9 T_{1/2} = 165 min). Once solubility is further improved, the series would appear suitable for *in vivo* efficacy testing studies.

Supplementary Material

Refer to Web version on PubMed Central for supplementary material.

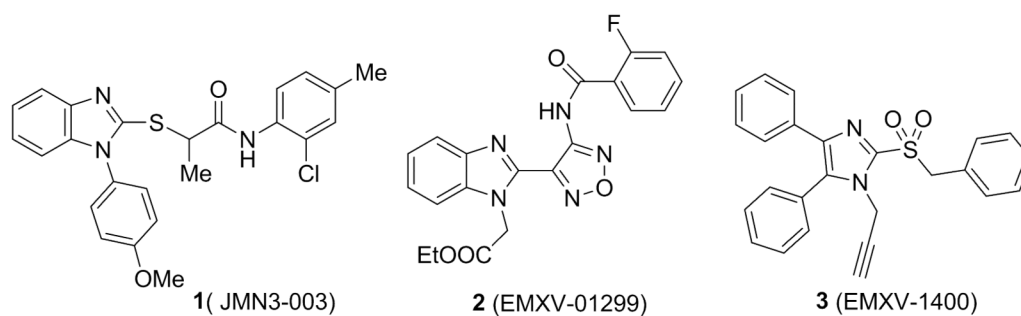
Acknowledgments

This work was supported, in part, by Public Health Service Grants AI071002 and AI057157 (to R. K. P.) from the NIH/NIAID.

REFERENCES

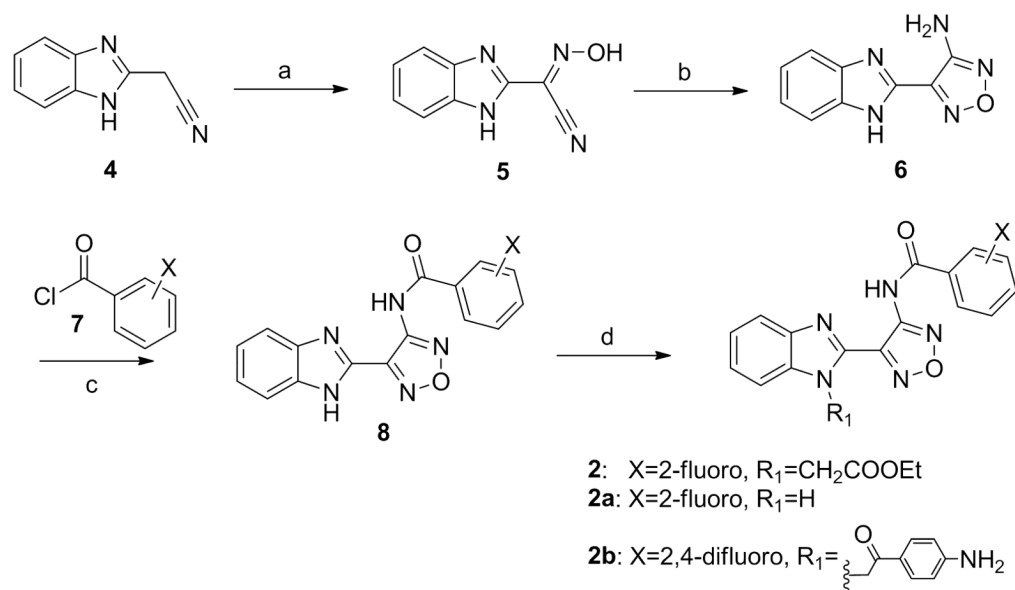
- (1). Organization, W. H.. World Health Statistics. 2013.
- (2). Why should influenza be a public health priority? *Vaccine*. 2012; 30:7418–7420. [PubMed: 23330160]
- (3). Watanabe T, Watanabe S, Kawaoka Y. Cellular Networks Involved in the Influenza Virus Life Cycle. *Cell Host Microbe*. 2010; 7:427–439. [PubMed: 20542247]
- (4). Konig R, Stertz S, Zhou Y, Inoue A, Hoffmann HH, Bhattacharyya S, Alamares JG, Tscherne DM, Ortigoza MB, Liang YH, Gao QS, Andrews SE, Bandyopadhyay S, De Jesus P, Tu BP, Pache L, Shih C, Orth A, Bonamy G, Miraglia L, Ideker T, Garcia-Sastre A, Young JAT, Palese P, Shaw ML, Chanda SK. Human host factors required for influenza virus replication. *Nature*. 2010; 463:813–817. [PubMed: 20027183]
- (5). Yoon JJ, Chawla D, Paal T, Ndungu M, Du YH, Kurtkaya S, Sun AM, Snyder JP, Plemper RK. High-throughput screening-based identification of paramyxovirus inhibitors. *J. Biomol. Screen*. 2008; 13:591–608. [PubMed: 18626114]
- (6). Moore TW, Sana K, Yan D, Thepchatri P, Ndungu JM, Saindane MT, Lockwood MA, Natchus MG, Liotta DC, Plemper RK, Snyder JP, Sun AM. Asymmetric synthesis of host-directed inhibitors of myxoviruses. *Beilstein J. Org. Chem*. 2013; 9:197–203. [PubMed: 23400228]

- (7). Sun AM, Ndungu JM, Krumm SA, Yoon JJ, Thepchatri P, Natchus M, Plemper RK, Snyder JP. Host-Directed Inhibitors of Myxoviruses: Synthesis and in Vitro Biochemical Evaluation. *ACS Med. Chem. Lett.* 2011; 2:798–803. [PubMed: 22328961]
- (8). Laufer SA, Hauser DRJ, Liedtke AJ. Regiospecific and highly flexible synthesis of 1,4,5-trisubstituted 2-sulfanylimidazoles from structurally diverse ethanone precursors. *Synthesis-Stuttgart.* 2008:253–266.
- (9). Guravaiah N, Rao VR. Stereoselective Synthesis of Substituted 2-(Z-Styrylsulfonyl)-ml-2013-00166b.R11h-Imidazoles and Benzothiazole. *Synthetic Commun.* 2010; 40:808–813.
- (10). Sugimoto H, Nakamura S, Watanabe Y, Toru T. Enantioselective hydrogen atom transfer to alpha-sulfonyl radicals controlled by selective coordination of a chiral Lewis acid to an enantiotopic sulfonyl oxygen. *Tetrahedron-Asymmetr.* 2003; 14:3043–3055.
- (11). Dodson RM, Ross F. The Preparation of 2-Alkylthioimidazoles. *J. Am. Chem. Soc.* 1950; 72:1478–1480.
- (12). Rao KVP, Sundaramurthy V. Regioselective Electrophilic Substitutions of 4h-Imidazo[2,1-C][1,4]Benzoxazine and 4h-Imidazo[2,1-C][1,4]Benzthiazine. *J. Org. Chem.* 1992; 57:2737–2739.
- (13). Zhou YR, Gong YF. Asymmetric Copper(II)-Catalysed Nitroaldol (Henry) Reactions Utilizing a Chiral C-1-Symmetric Dinitrogen Ligand. *Eur. J. Org. Chem.* 2011:6092–6099.
- (14). Krumm SA, Ndungu JM, Yoon JJ, Dochow M, Sun AM, Natchus M, Snyder JP, Plemper RK. Potent Host-Directed Small-Molecule Inhibitors of Myxovirus RNA-Dependent RNA-Polymerases. *Plos. One.* 2011:6.

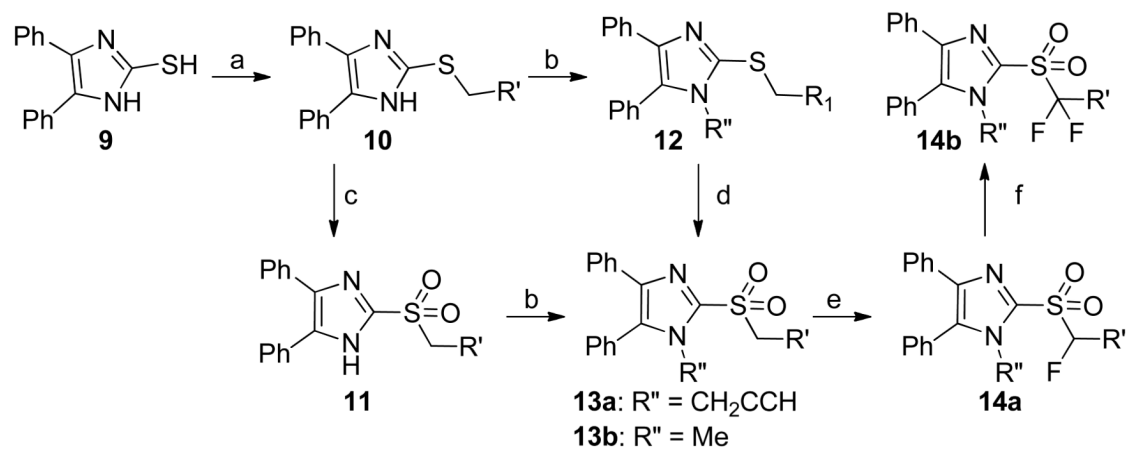


Cmpd	Influenza A/sw/ Texas/2009 (H1N1) EC ₅₀ [μM]	Influenza A/Aichi/ 1968 (H3N2) EC ₅₀ [μM]	RSV EC ₅₀ [μM]	Cytotox. CC ₅₀ [μM]	Specificity Index SI (CC ₅₀ /EC ₅₀)
1	0.04	ND	0.07	>50	>1,250 _{IFA/Texas}
2	0.1 (0.07-0.17)	0.05 (0.03-0.07)	0.14 (0.12-0.17)	>50	>500 _{IFA/Texas}
3	0.2 (0.15-0.3)	0.92 (0.48-1.76)	0.45 (0.36-0.55)	>50	>250 _{IFA/Texas}

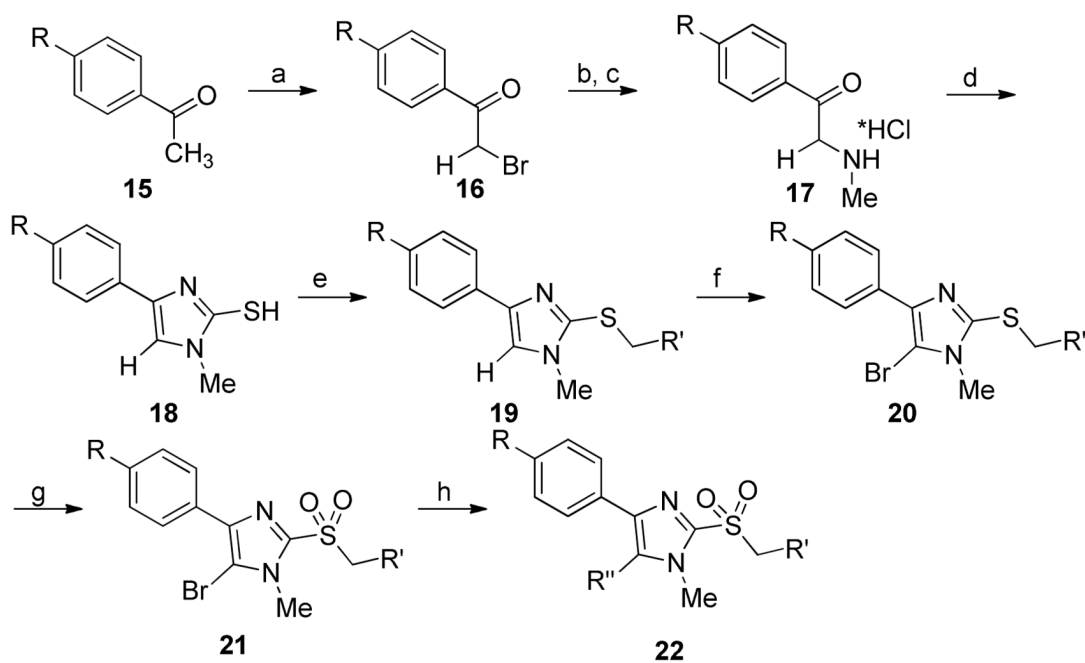
Figure 1.
Structures of host-directed anti-virals and their biological profiles.

**Scheme 1^a**

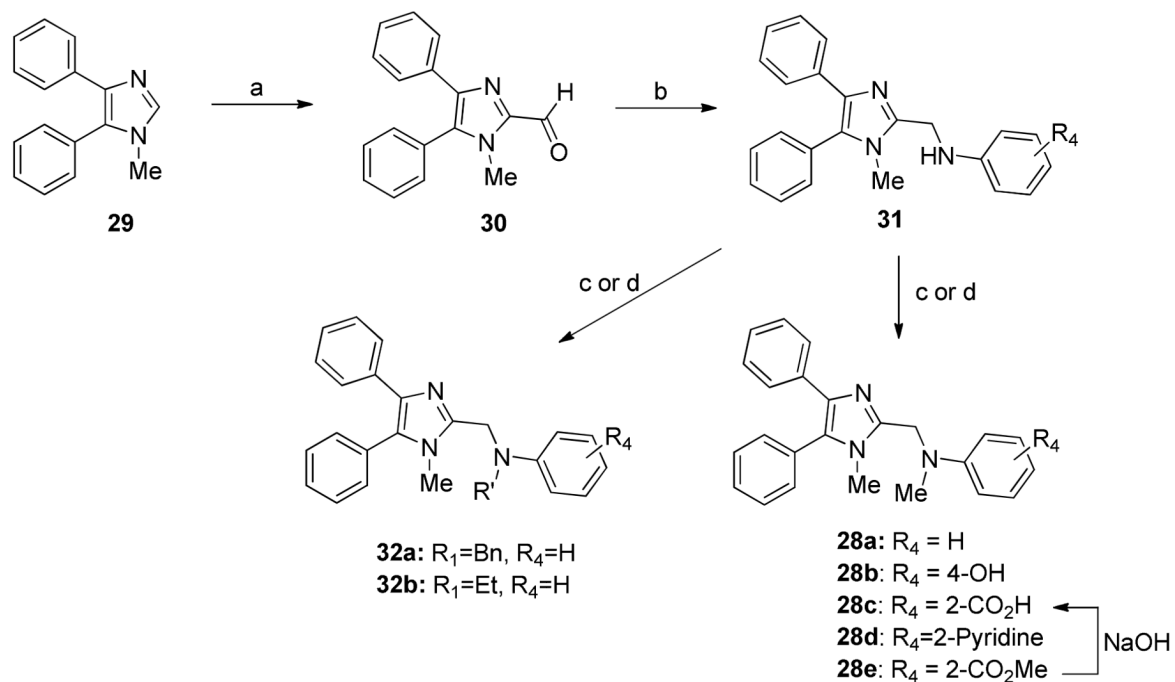
^aReagents and conditions: (a) NaNO₂, AcOH-H₂O. (b) NH₂OH-HCl/KOH, CH₃(CH₂OCH₂)₃CH₃-H₂O. (c) **7**, ^tPr₂NEt/THF, then KOH-CH₃OH. (d) 2-bromoethyl acetate, ^tPr₂NEt/THF.

**Scheme 2^a**

^aReagents and conditions: (a) R'CH₂Br, Cs₂CO₃, DMF. (b) R''X, Cs₂CO₃, DMF. (c) H₂O₂/AcOH. (d) *m*-chloroperoxybenzoic acid, CH₂Cl₂. (e) KO^tBu, *N*-fluorobenzenesulfonimide, THF. (f) LiN(SiMe₃)₂, *N*-fluorobenzenesulfonimide, THF.

**Scheme 3^a**

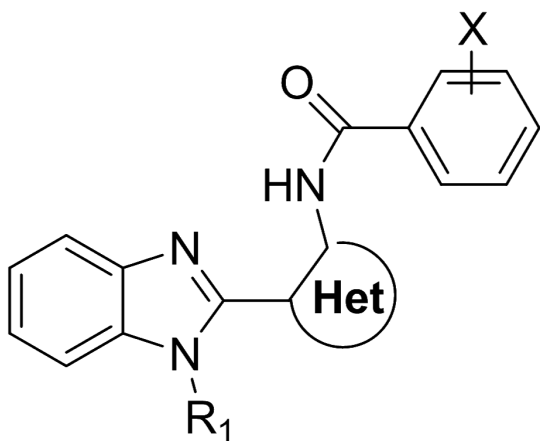
^aReagents and conditions: (a) Br₂, AcOH. (b) NH₂Me, CH₂Cl₂. (c) HCl, MeOH. (d) NaSCN, DMF, 160 °C. (e) BrCH₂R', Cs₂CO₃, DMF. (f) *N*-bromosuccinimide, CCl₄. (g) *m*-chloroperoxybenzoic acid, CH₂Cl₂. (h) R''B(OH)₂, Na₂CO₃, Pd(PPh₃)₄.

**Scheme 4^a**

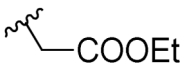
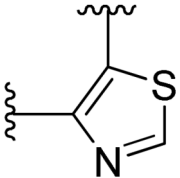
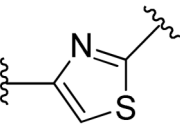
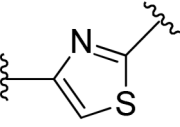
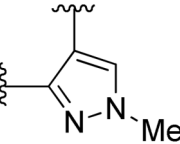
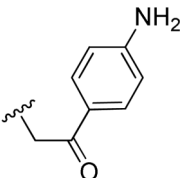
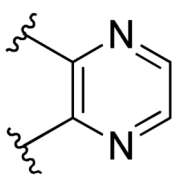
^aReagents and conditions: (a) $t\text{BuLi}/\text{DMF}$, $-78\text{ }^\circ\text{C}$. (b) aniline/ CH_2Cl_2 , then $\text{NaBH}(\text{OAc})_3$, 16h. (c) HCHO (37% in H_2O)/ CH_2Cl_2 , then $\text{NaBH}(\text{OAc})_3$, 16h. (d) LiHMDS , RX , THF .

Table 1

Analogues of hit series 2.

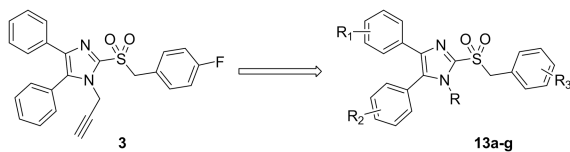


Cmpd	R ₁	Het	X	EC ₅₀ (μM) ^a	
				Influenza A/WSN(H1N1)	MeV-Edm
2			2-fluoro	0.012 (0.012-0.013)	0.023 (0.019-0.028)
2a	H		2-fluoro	>10	>10
2b			2-fluoro	0.7	0.4

Cmpd	R ₁	Het	X	EC ₅₀ (μM) ^a	
				Influenza A/WSN(H1N1)	MeV-Edm
2c			2,6-fluoro	~10	~10
2d	iPr		2,6-difluoro	4.0	~10
2e	-CH ₂ COOH		2,6-difluoro	>10	>10
2f	H		2-fluoro	>10	>10
2g			H	>10	>10

^a50% inhibitory concentration were calculated using the variable slope (four parameters) non linear regression-fitting algorithm embedded in the Prism 5 software package (GraphPad Software). Values represent averages of four assessments; highest concentration assessed, 10 μM.

Table 2

Anti-viral EC₅₀ values for selected sulfone analogs

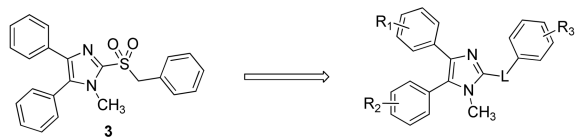
Cmpd	R, R ₁ , R ₂ , R ₃	EC ₅₀ (η M) ^a		S9 stability T _{1/2} (min)	
		Influenza	MeV	human	hamster
3	-	0.5	0.74	19	<2.5
13a	R=H R ₁ =R ₂ =R ₃ =H	>10	>10	14	<2.5
13b	R=Me R ₁ =R ₂ =R ₃ =H	0.3	4.0	2-12 ^b	<2.5 ^b
13c	R=Me R ₁ =R ₂ =R ₃ =p-F	>10	>10	<2.5 ^b	<2.5 ^b
13d	R=Et R ₁ =R ₂ =R ₃ =H	2.0	1.0	ND ^c	ND ^c
13e	R=Bn R ₁ =R ₂ =R ₃ =H	10	>10	ND ^c	ND ^c
13f	R=allyl R ₁ =R ₂ =H, R ₃ =p-F	4.2	4.6	ND ^c	ND ^c
13g	R=Me R ₁ =R ₂ =H, R ₃ =4-py	>10	>10	ND ^c	ND ^c
13h	R=Me R ₁ =R ₂ =H, R ₃ =3-py	>10	9	ND ^c	ND ^c
22a	R=Me; R ₁ = R ₃ =p-F; R ₂ =4-py	>10	>10	ND ^c	ND ^c
22b	R=Me, R ₁ =R ₃ = p-F; R ₂ =3-py	>10	>10	ND ^c	ND ^c

^a50% inhibitory concentration were calculated using the variable slope (four parameters) non-linear regression-fitting algorithm embedded in the Prism 5 software package (GraphPad Software). Values represent averages of four assessments; highest concentration assessed, 10 μ M.

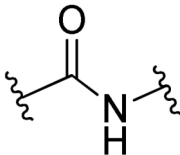
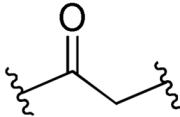
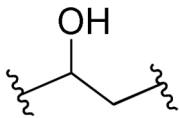
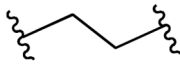
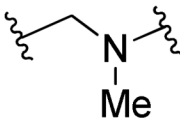
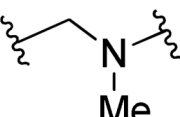
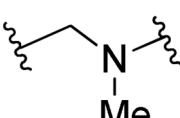
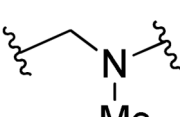
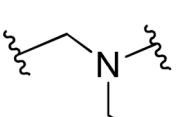
^bValues represent the range of two experiments carried out on different dates. Where only one value is given, the half-lives were calculated to be the same.

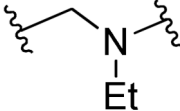
^cNot determined (ND) when EC₅₀>10 μ M

Table 3

Analogues of **3** containing different linker moieties.

Cmpd	L	R ₁ , R ₂ , R ₃	EC ₅₀ (μM) ^b		S9 stability T _{1/2} (min)	
			Influenza	MeV	human	hamster
3	-	-	0.5	0.74	19	<2.5
12		R ₁ =R ₂ =R ₃ =4-H	0.4	6.0	15	3
14a		R ₁ =R ₂ =R ₃ =4-F	8.0	5.0	<2.5	<2.5
14b		R ₁ =R ₂ =R ₃ =H	>10	>10	ND ^c	ND
15		R ₁ =R ₂ =R ₃ =4-F	>10	>10	>90	54
23^a		R ₁ =R ₂ =R ₃ =H	>10	>10	27	<2.5
24a		R ₁ =R ₂ =H, R ₃ =2-F	10.0	9.0	ND	ND

Cmpd	L	R ₁ , R ₂ , R ₃	EC ₅₀ (μM) ^b		S9 stability T _{1/2} (min)	
			Influenza	MeV	human	hamster
24b		R ₁ =R ₂ =H, R ₃ =2-NO ₂	6.0	9.0	ND	ND
25		R ₁ =R ₂ =R ₃ =H	10	>10	>90	5
26		R ₁ =R ₂ =R ₃ =H	>10	>10	ND	ND
27		R ₁ =R ₂ =R ₃ =H	10.0	6.0	ND	ND
28a		R ₁ =R ₂ =R ₃ =H	0.88	0.91	165	<5.0
28b		R ₁ =R ₂ =H, R ₃ =4-OH	10	10	ND	ND
28c		R ₁ =R ₂ =H, R ₃ =2-COOH	3	3	ND	ND
28d		R ₁ =R ₂ =H, R ₃ =2-Py	10	10	ND	ND
32a		R ₁ =R ₂ =R ₃ =H	>10	>10	ND	ND

Cmpd	L	R ₁ , R ₂ , R ₃	EC ₅₀ (μM) ^b		S9 stability T _{1/2} (min)	
			Influenza	MeV	human	hamster
32b		R ₁ =R ₂ =R ₃ =H	10	10	ND	ND

^aLacks 1-methyl group on imidazole ring.

^b50% inhibitory concentration were calculated using the variable slope (four parameters) non-linear regression-fitting algorithm embedded in the Prism 5 software package (GraphPad Software). Values represent averages of four assessments; highest concentration assessed, 10 μM.

^cNot determined when EC₅₀ >10 μM.